Three-dimensional reconstruction of the Golgi apparatus in osteoclasts by a combination of NADPase cytochemistry and serial section scanning electron microscopy

Tsuneyuki Yamamoto[1], Tomoka Hasegawa[2], Hiromi Hongo[2], Norio Amizuka[2]

[1] Department of Functional Anatomy, Hokkaido University Graduate School of Dental Medicine

[2] Department of Developmental Biology of Hard Tissue, Hokkaido University Graduate School of Dental Medicine

Corresponding author:

Tsuneyuki Yamamoto (ORCID: 0000-0001-5247-2884)

Department of Functional Anatomy, Hokkaido University Graduate School of Dental Medicine, Kita 13 Nishi 7, Kita-ku, Sapporo 060-8586, Japan

E-mail: yamatsu@den.hokudai.ac.jp

Tel: +81-11-706-4219

Fax: +81-11-706-4928

Abstract

The three-dimensional morphology of the Golgi apparatus in osteoclasts was investigated by computer-aided reconstruction. Rat femora were treated for nicotinamide adenine dinucleotide phosphatase (NADPase) cytochemistry, and light microscopy was used to select several osteoclasts in serial semi-thin sections to investigate the Golgi apparatus by backscattered electron-mode scanning electron microscopy. Lace-like structures with strong backscattered electron signals were observed around the nuclei. These structures, observed within the Golgi apparatus, were attributed to the reaction products (*i.e.*, lead precipitates) of NADPase cytochemistry. Features on the images corresponding to the Golgi apparatus, nuclei, and ruffled border were manually traced and three dimensionally reconstructed using ImageJ/Fiji (an open-source image processing package). In the reconstructed model, the Golgi apparatus formed an almost continuous structure with a basket-like configuration, which surrounded all the nuclei and also partitioned them. This peculiar three-dimensional morphology of the Golgi apparatus was discovered for the first time in this study. On the basis of the location of the *cis*- and *trans*-sides of the Golgi apparatus and the reported results of previous studies, we postulated that the nuclear membrane synthesized specific proteins in the osteoclasts and accordingly the Golgi apparatus accumulated around the nuclei as a receptacle.

195 words

Key words: Golgi apparatus, NADPase, Osteoclasts, Scanning electron microscopy.

Introduction

Osteoclasts are large multinuclear cells that participate in bone formation and remodeling in concert with osteoblasts and osteocytes. The main function of osteoclasts is to remove the inorganic and organic matrices of bone by secreting acid and lysosomal or organic matrix-degrading enzymes. To produce and isolate abundant lysosomes, osteoclasts develop the Golgi apparatus, which encompasses the nucleus. The Golgi apparatus generally faces the nucleus with its *cis*-side and partitions two adjoining nuclei with the *cis*-side facing one nucleus or with clear loss of *cis–trans* polarity (Baron et al. 1988; Noda et al. 1991; Yamamoto et al. 2019). The following findings on the three-dimensional structure of the Golgi saccules in osteoclasts were obtained by scanning electron microscopy using an osmium maceration method: 1) The *cis*-most saccule shows a sieve-like configuration with fine fenestrations. 2) The saccules have decreasing fenestration numbers and display a more plate-like appearance toward the *trans*-side. 3) The three-dimensional structure of the Golgi saccules is comparable to that generally seen in other cell types (Yamamoto et al. 2019).

The three-dimensional extension or overall shape of the Golgi apparatus is widely considered a single continuous structure in many cell types (Novikoff et al. 1971; Rambourg et al. 1974, 1984, 1992; Dylewsky et al. 1984; Noda and Ogawa 1984; Tanaka et al. 1986; Tanaka and Fukudome 1991; Tamaki and Yamashina 1997) even though the Golgi apparatus is scattered within the cells in thin histological sections. Recently, Koga et al. (2016, 2017) confirmed the structural continuity of the Golgi apparatus by using a novel imaging technique, that is, serial section scanning electron microscopy or array tomography using the backscattered electron mode. However, the three-dimensional extension of the Golgi apparatus has not yet been sufficiently characterized in osteoclasts, although their Golgi apparatus is also assumed to form a unified structure (Yamamoto et al. 2019).

There is a consensus that the overall shape of the Golgi apparatus is associated with the function of cells (Clermont et al. 1995; Mogelsvang et al. 2004; Tanaka and Fukudome 1991; Watanabe et al. 2014; Koga et al. 2016, 2017). Hence, to gain a deeper understanding of osteoclast biology, the three-dimensional morphology of the Golgi apparatus should be elucidated in osteoclasts. For this purpose, osteoclasts were examined in the growing femora of rats by a combination of nicotinamide adenine dinucleotide phosphatase (NADPase) cytochemistry, which is localized in the middle Golgi saccules (Smith 1980; Parsons and Smith 1984; Rambourg et al. 1984, 1987, 1988; Rambourg and Clermont 1986; Bennett and Hemming 1989; Hermo et al. 1991), and serial section scanning electron microscopy (Koga et al. 2016, 2017).

Materials and Methods

Eight-week-old male Wistar rats were used. The animals were treated in accordance with the guidelines of the Hokkaido University Experimental Animal Committee (Approval No. 10-0081 and 15-0041).

NADPase cytochemistry

The animals were anesthetized with an intraperitoneal injection of sodium pentobarbital and perfused with 2.5% glutaraldehyde in 0.06 M cacodylate buffer (pH 7.4). The distal half of the femora was dissected out, immersed in the same fixative overnight, and decalcified in 5% EDTA (pH 7.4) for 3 weeks. Then, the specimens were longitudinally cut into slices of 200–300 μm in thickness, including the growth plate, with a blade. These slices were treated for NADPase cytochemistry in accordance with previous studies (Smith 1980; Parsons and Smith

1984). Briefly, the slices were incubated in medium containing 4 mM β-$NADP^+$(Oriental Yeast Co., Ltd., Tokyo, Japan), 4 mM lead acetate, and 5% sucrose in 40 mM sodium acetate buffer (pH 5.0) for 2–3 h at 37°C. After incubation, they were treated with a 1% ammonium sulfide solution. Controls were incubated in duplicate without the substrate for cytochemistry.

The slices were postfixed with 1% OsO_4 and 1.5% potassium ferrocyanide in 0.06 M cacodylate buffer (pH 7.4) for 1 h. After dehydration in a graded series of acetone solutions, the specimens were embedded in EPON 812. From some tissue blocks, serial 0.5-μm-thick sections were prepared for light microscopy and serial section scanning electron microscopy, as described below. From the other tissue blocks, ultrathin sections were prepared and stained with uranyl acetate and lead citrate for examination under a JEM-1400 transmission electron microscope at an accelerating voltage of 80kv.

Serial section scanning electron microscopy

Approximately 20–30 serial semi-thin sections were mounted on each glass slide. Under a Nikon ECLIPSE 80*i* microscope with an immersion lens (100x/1.25 (N.A)), the primary trabeculae adjacent to the growth plate were examined and several active osteoclasts, which could be traced within 32-40 serial sections, were selected. Images were captured with a Qimaging-Micropublisher 5.0 camera with a resolution of 2560 x 1920 pixels and 24bit color for the Image-Pro premier software version 9 (Media Cybernetics Co., Ltd., Rockville, U.S.A). Serial section scanning electron microscopy after sectioning was fundamentally based on the original procedure by Koga et al. (2016, 2017). After the sections were stained with uranyl acetate and lead citrate, the glass slides with the sections were cut into small pieces and mounted on aluminum stabs with carbon tape. The sections were then coated with platinum-palladium prior to examination under a Hitachi S-4800 scanning electron microscope equipped with a TTL detector for detection of backscattered electrons. The selected osteoclasts were observed by backscattered electron-mode at an accelerating voltage of 15 KV. Images of 1280 x 960 pixels were captured at magnifications of 1500(66.1 nm /pixel), 5000(19.8 nm/pixel), and 10000 (9.9nm/pixel) and saved as bitmap image for three-dimensional reconstruction.

Three-dimensional reconstruction

Saved images of the osteoclasts were black and white reversed. Images of a magnification of 1500 were loaded into ImageJ/Fiji (Schindelin et al. 2012) using Image Sequence (an import tool in ImageJ/Fiji), and automatically aligned using StackReg (an alignment tool). The serial aligned images were transferred to Microsoft PowerPoint and the nuclei, Golgi apparatus, and ruffled border were manually traced and colored on the images (for details, see below). Then the original images were converted to the black background. The PowerPoint images were saved as JPEG file format (jpg) and again loaded into ImageJ/Fiji. After size or thickness adjustment, the three components were reconstructed using 3D viewer (a reconstruction tool).

Results and Discussion

Localization and backscattered electron image of lead precipitates after NADPase cytochemistry

Lead precipitates, the reaction products of NADPase cytochemistry were observed in the nuclei, the Golgi apparatus, and vesicular organelles indicative of lysosomes under a transmission electron microscope (Fig.1a-c). Moreover,

lead precipitates were observed on the bone surfaces other than bone surfaces covered by the ruffled border (Fig. 1c, d). However, the lead precipitates on the bone surfaces were probably false reaction products because they were also observed in the controls (not shown). By backscattered electron-mode scanning electron microscopy, the lead precipitates were detected as intense backscattered electron signals. On the basis of transmission electron microscopic findings, lace- or strand-like structures around the nuclei were regarded as the Golgi apparatus (Figs. 2 and 3a). On the other hand, vesicular structures were excluded despite high signal intensity because they might be other organelles, e.g., lysosomes and lysosome derivatives. Unidentifiable structures were also excluded. The distinction was finalized by images of magnifications of 5000 and 10000. As mentioned above, the bone surfaces without lead precipitates or backscattered electron signals corresponded to the portions of the ruffled border. Through these procedures, the nuclei, Golgi apparatus, and ruffled border were determined and traced (Fig. 3b, c).

Three-dimensional extension of the Golgi apparatus

The reconstructed model showed that the middle Golgi saccules extended around the nuclei with a net-like configuration. The model was rotated and viewed from various directions. With only a few exceptions, the Golgi apparatus formed a single continuous structure with a porous, basket-like configuration and wrapped all the nuclei (Fig. 4a and b). The model was randomly cut, and the sections were examined. The Golgi apparatus was found to partition any two nuclei (Fig. 4c). From these findings, the following conclusions were made for the three-dimensional extension of the Golgi apparatus in osteoclasts: 1) The Golgi apparatus forms a single unified structure with a basket-like configuration. 2) The network of the Golgi apparatus wraps all of nuclei. 3) The Golgi apparatus separates each nucleus within the basket-like structure. In support of feature 1), there is an agreement that the Golgi apparatus is continuous in many types of mononuclear cells, such as neurons, mucous cells, mammary epithelial cells, pancreatic and parotid acinar cells, and pituitary endocrine cells (Novikoff et al. 1971; Rambourg et al. 1974, 1984, 1992; Dylewsky et al. 1984; Noda and Ogawa 1984; Tanaka et al. 1986; Tanaka and Fukudome 1991; Tamaki and Yamashina 1997; Koga et al. 2016, 2017). We proposed a similar structure for the Golgi apparatus in osteoclasts in a previous study (Yamamoto et al. 2019). This study established that the Golgi apparatus also maintained structural continuity in osteoclasts despite the structure extending around multiple nuclei and wrapping all of them.

Relationship between the Golgi apparatus and nuclei

The three-dimensional extension of the Golgi apparatus does not surround the nucleus of mononuclear cells other than neurons, that is, ganglion cells and Purkinje cells (Rambourg et al. 1974; Rambourg and Clermont 1986; Koga et al. 2017). In almost all cells, the Golgi apparatus is located a short distance from the nucleus, not surrounding it. In addition, the *cis*- and *trans*-sides of the Golgi apparatus are located at different positions between osteoclasts and other cell types. Watanabe et al. (2014) investigated the overall shape and function of the Golgi apparatus in pituitary gland and pancreatic acinar cells. Briefly, the Golgi apparatus can be divided into three types, that is, cap-shaped Golgi (mammotrope and somatotrope), ball-shaped Golgi (gonadotrope and thyrotrope), and cup-shaped Golgi (pancreatic acinar cell). In all types, the *cis*- and *trans*-sides of the Golgi apparatus are located on the outside and inside surfaces of the three-dimensional structure, respectively. Rough endoplasmic reticulum supplies precursor proteins to the *cis*-most saccule. The proteins are maturated as they are trafficked toward the *trans*-side or inward and are released into the inner space. Then, the secretory vesicles are transferred outward in the opposite direction

through gaps or pores and finally secreted extracellularly.

In osteoclasts, the positions of the *cis*- and *trans*-sides of the Golgi apparatus are reversed, that is, the *cis*- and *trans*-sides are located on the inside and outside surfaces of the basket-like structure, respectively (Baron et al. 1988; Noda et al. 1991; Yamamoto et al. 2019). In addition, the nucleus, not the endoplasmic reticulum, is located close to the *cis*-most saccule. Hence, the secretory process of osteoclasts may differ from that mentioned above. On the basis of the observed high arylsulfatase activity, Baron et al. (1985, 1988, 1990) proposed that the nuclear membrane is involved in enzyme-producing processes. Because of the ribosome-like particles on the nuclear membrane and the proximity of the Golgi apparatus to the nuclei, we also suggested that the nuclear membrane participated in the secretory process in osteoclasts (Yamamoto et al. 2019). Briefly, during active bone resorption, lysosomes, phagosomes, and vacuoles likely circulate vigorously in the cytoplasm of osteoclasts. Under these circumstances, the normal protein-secreting route from the rough endoplasmic reticulum to the Golgi apparatus cannot presumably function properly. Instead, the nuclear membrane may synthesize specific proteins, such as arylsulfatase, sialyltransferase, and 100 kD lysosomal membrane protein (Baron et al. 1985, 1988, 1990), and accordingly the Golgi apparatus accumulates around the nuclei as a receptacle. We postulated this mechanism on the basis of features 2) and 3) of the three-dimensional extension of the Golgi apparatus, as specified in the previous section.

The ruffled border was also reconstructed, in this study, to examine the relationship between the morphology of Golgi apparatus and the position of the ruffled border (Fig.5). The Golgi apparatus did not appear to alter the morphology of the ruffled border with respect to its position. Because this study included manual and subjective procedures, we intend to investigate this issue further using more elaborate equipment and techniques.

Acknowledgements

We thank Edanz (https://jp.edanz.com/ac) for editing a draft of this manuscript.

Author contributions

TY, as the main researcher, was involved in all the processes of this study, in particular, cytochemical treatment, electron microscopic observation, and computer-aided reconstruction. TH and HH prepared the samples, including fixation, resin embedding, and sectioning. NA participated in the discussion and preparation of the manuscript. All the above authors have read and agreed to the submission of the manuscript.

Funding

This study was supported by a grant from the Japanese Society for the Promotion of Science to T. Yamamoto (No. 22592028).

Data availability

The datasets generated and analyzed during the current study are available from the corresponding author on reasonable request.

Compliance with ethical standards

Conflict of interest

We declare no conflicts of interest.

References

Baron R, Neff L, Louvard D, Courtoy P J (1985) Cell-mediated extracellular acidification and bone resorption: evidence for a low pH in resorbing lacunae and localization of a 100-KD lysosomal membrane protein at the osteoclast ruffled border. J Cell Biol 101: 2210-2222

Baron R, Neff L, Brown W, Courtoy P J, Louvard D, Farqunhar M G (1988) Polarized secretion of lysosomal enzymes: co-distribution of cation-independent mannose-6-phosphate receptors and lysosomal enzymes along the osteoclast exocytotic pathway. J Cell Biol 106: 1863-1872

Baron R, Neff L, Brown W, Louvard D, Courtoy P J (1990) Selective internalization of the apical plasma membrane and rapid redistribution of lysosomal enzymes and mannose-6-phosphata receptors during osteoclast inactivation by calcitonin. J Cell Sci 97: 439-447

Bennet G, Hemming R (1989) Ultrastructural localization of CMPase, TPPase, and NADPase activity in neurons, satellite cells, and Schwann cells in frog dorsal root ganglia. J Histochem Cytochem 37: 165-172.

Clermont Y, Rambourg A, Hermo L (1995) Trans-Golgi network (TGN) of different cell types: three-dimensional structural characteristics and variability. Anat Rec 242:289-301

Dylewsky D P, Maralick R M, Keenan T W (1984) Three-dimensional ultrastructure of the Golgi apparatus in bovine mammary epithelial cells during lactation. J Ultrastr Res 87: 75-85

Hermo L, Green H, Clermont Y (1991) Golgi apparatus of epithelial principal cells of the epididymal initial segment of the rat: structure, relationship with endoplasmic reticulum, and role in the formation of secretory vesicles. Anat Rec 229: 159-176

Koga D, Kusumi S, Ushiki T (2016) Three-dimensional shape of the Golgi apparatus in different cell types: serial section scanning electron microscopy of the osmium-impregnated Golgi apparatus. Microscopy 65:145-157

Koga D, Kusumi S, Ushiki T, Watanabe T (2017) Integrative method for three-dimensional imaging of the entire Golgi apparatus by combining thiamine pyrophosphatase cytochemistry and array tomography using backscattered electron-mode scanning electron microscopy. Biomed Res 38:285-296

Mogelsvang S, Marsh B R, Ladinsky M S, Howell K E (2004) Predicting function from structure: 3D structure studies of the mammalian Golgi complex. Traffic 5: 338-345

Noda K, Nakamura Y, Wakimoto Y, Tanaka T, Kuwahara Y (1991) Thiamine pyrophosphatase activity in the Golgi apparatus of calcitonin-treated osteoclasts. J Electron Microsc 40:399-402

Noda T, Ogawa K (1984) Golgi apparatus is one continuous organelle in pancreatic exocrine cell of mouse. Acta Histochem Cytochem 17: 435-451

Novikoff PM, Novikoff AB, Quintana N, Hauw J-J (1971) Golgi apparatus, GERL, and lysosomes of neurons in rat dorsal root ganglia, studied by thick section and thin section cytochemistry. J Cell Biol 50:859-886

Parsons S M, Smith C E (1984) Ultrastructural localization of nicotinamide adenine dinucleotide phosphatase (NADPase) activity within columnar, goblet, and Paneth cells of rat small intestine. J Histochem Cytochem 32: 989-997

Rambourg A, Clermont Y, Marraud A (1974) Three-dimensional structure of the osmium-impregnated Golgi apparatus as seen in the high voltage electron microscope. Am J Anat 140: 27-46.

Rambourg A, Clermont Y (1986) Tridimensional structure of the Golgi apparatus in type A ganglion cells of the rat. Am J Anat 176: 393-409

Rambourg A, Clermont Y, Hermo L, Segretain D (1987) Tridimensional architecture of the Golgi apparatus and its components in mucous cells of Brunner's Glands of the mouse. Am J Anat 179: 95-107

Rambourg A, Clermont Y, Hermo L (1988) Formation of secretion granules in the Golgi apparatus of pancreatic acinar cells of the rat. Am. J. Anat. 183: 187-199.

Rambourg A, Clermont Y, Chrétien M, Oliver L (1992) Formation of secretory granules in the Golgi apparatus of prolactin cells in the rat pituitary gland: a stereoscopic study. Anat. Rec. 232: 169-179.

Rambourg A, Segretain D, Clermont Y (1984) Tridimensional architecture of the Golgi apparatus in the atrial muscle cells of the rat. Am J Anat 170: 163-179

Schindelin J, Arganda-Carreras I, Frise E, Kaynig V, Longair M, Pietzsch T, Preibisch S, Rueden C, Saalfeld S, Schmid B, Tinevez J-Y, White DJ, Hartenstein V, Eliceiri K, Tomancak P, Cardona A (2012) Fiji: an open-source platform for biological-image analysis. Nat Methods 9: 676-682

Smith C E (1980) Ultrastructural localization of nicotinamide adenine dinucleotide phosphatase (NADPase) activity to the intermediate saccules of the Golgi apparatus in rat incisor ameloblasts. J Histochem Cytochem 28: 16-26

Tamaki H, Yamashina S (1997) Three-dimensional dynamics of the Golgi apparatus in mitotic parotid acinar cells: computer-aided reconstruction from cytochemically-marked ultrathin serial sections. Acta Histochem Cytochem 30: 643-651

Tanaka K, Fukudome H (1991) Three-dimensional organization of the Golgi complex observed by scanning electron microscopy. J Electron Microsc Tech 17: 15-23

Tanaka K, Mitsushima A, Fukudome H, Kashima Y (1986) Three-dimensional architecture of the Golgi complex observed by high resolution scanning electron microscopy. J Submicrosc Cytol 18: 1-9.

Watanabe T, Bochimoto H, Koga D, Hosaka M, Ushiki T (2014) Functional implications of the Golgi and microtubular network in gonadotropes. Mol. Cell Endocrinol. 385: 88-96.

Yamamoto T, Hasegawa T, Hongo H, Amizuka N (2019) Three-dimensional morphology of the Golgi apparatus in osteoclasts: NADPase and arylsulfatase cytochemistry, and scanning electron microscopy using osmium maceration. Microscopy 68:243-253

Figure Legends

Fig. 1 Transmission electron micrographs (**a–c**) and light micrograph (**d**) showing osteoclasts treated for NADPase cytochemistry. **a** The Golgi apparatus (arrowheads) surrounds the nuclei. **b** Magnification of the box in **a**. Lead precipitates in the Golgi apparatus are marked by arrowheads. **c and d** Lead precipitates (arrows) are observed on the bone surface covered by the clear zone (CZ) and the exposed bone surface but not on the bone surfaces covered by the ruffled border (RB). Bars = 2 μm (**a, c**), 0.5 μm (**b**)**,** and 3 μm (**d**).

Fig. 2 a By backscattered electron-mode scanning electron microscopy the Golgi apparatus (arrowheads) shows lace-like appearance near the nucleus (N). **b** Black and white reversed image of **a**. Bars = 0.5 μm.

Fig. 3 a Black and white reversed image of an osteoclast. The Golgi apparatus (arrowheads) is shown as black lines. Arrows indicate the positions of the ruffled border (see Fig.1c, d). **Inset.** Magnification of the box. The Golgi apparatus with lace-like appearance (arrowheads). **b** Reduction of **a**. Nuclei (blue), Golgi apparatus (yellow), and ruffled border (purple) are colored on the image. **c** The original image was converted to the black background. Bars = 2 μm (**a**), 1μm **(inset** in **a**), and 4 μm (**b**).

Fig. 4 a and b Reconstructed Golgi apparatus (yellow) and five nuclei (blue). **b** is the other side of **a**. Although there are a few isolated pieces (arrowheads), the Golgi apparatus forms an almost continuous and single structure and wraps all the nuclei. **c** One of the randomly cut sections. The Golgi apparatus partitions two nuclei.

Fig. 5 Reconstructed Golgi apparatus (yellow), nuclei (blue), and ruffled border (purple). Pairs (**a**, **b**) and (**c**, **d**) are the same osteoclasts. **b** and **d** are the other sides of **a** and **c**, respectively.

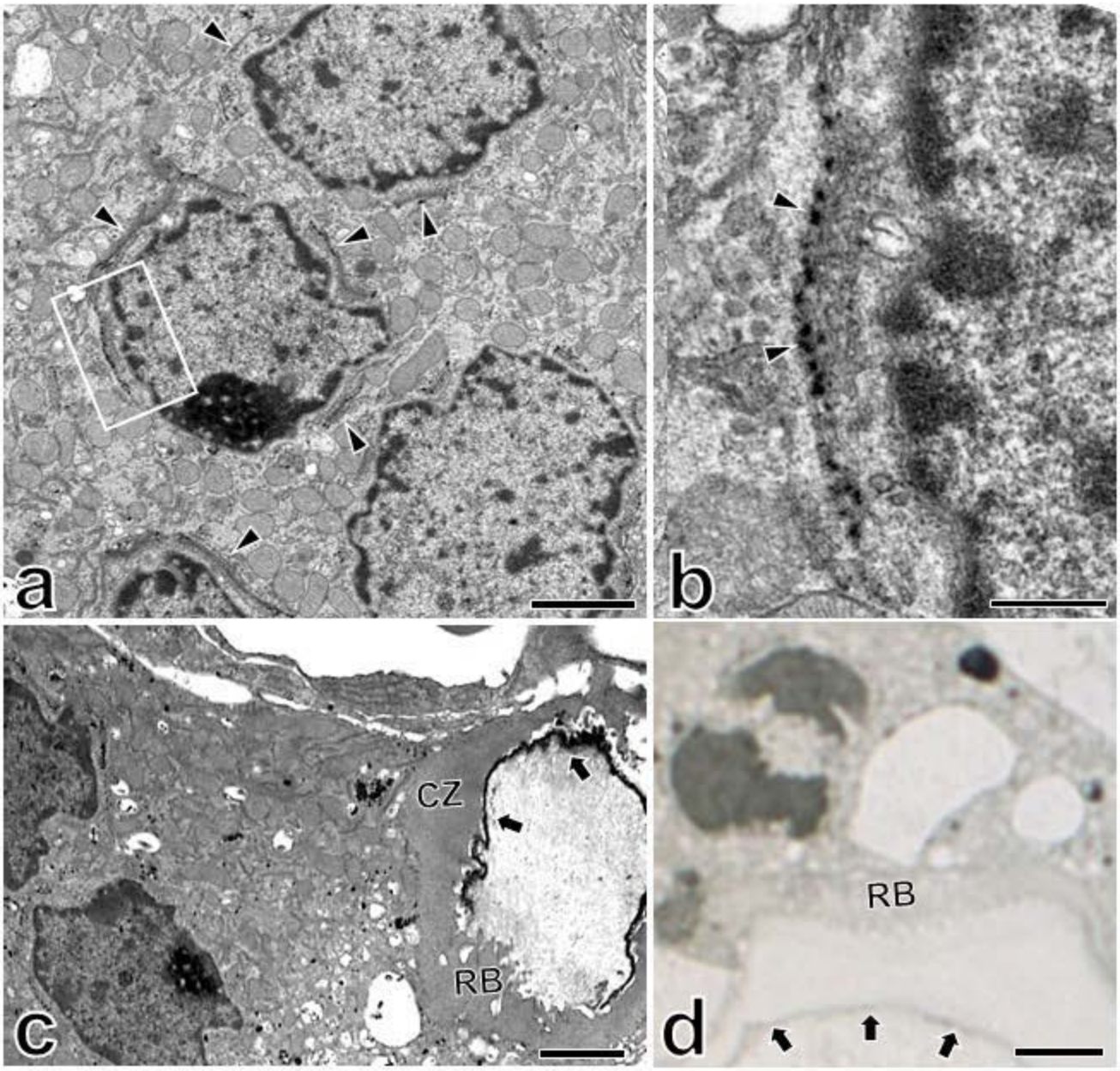

Fig.1

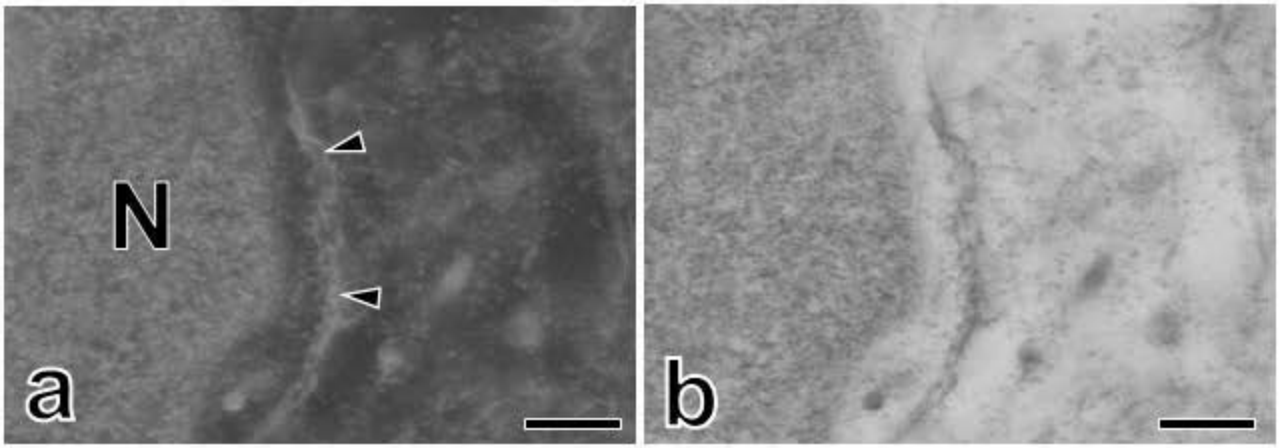

Fig.2

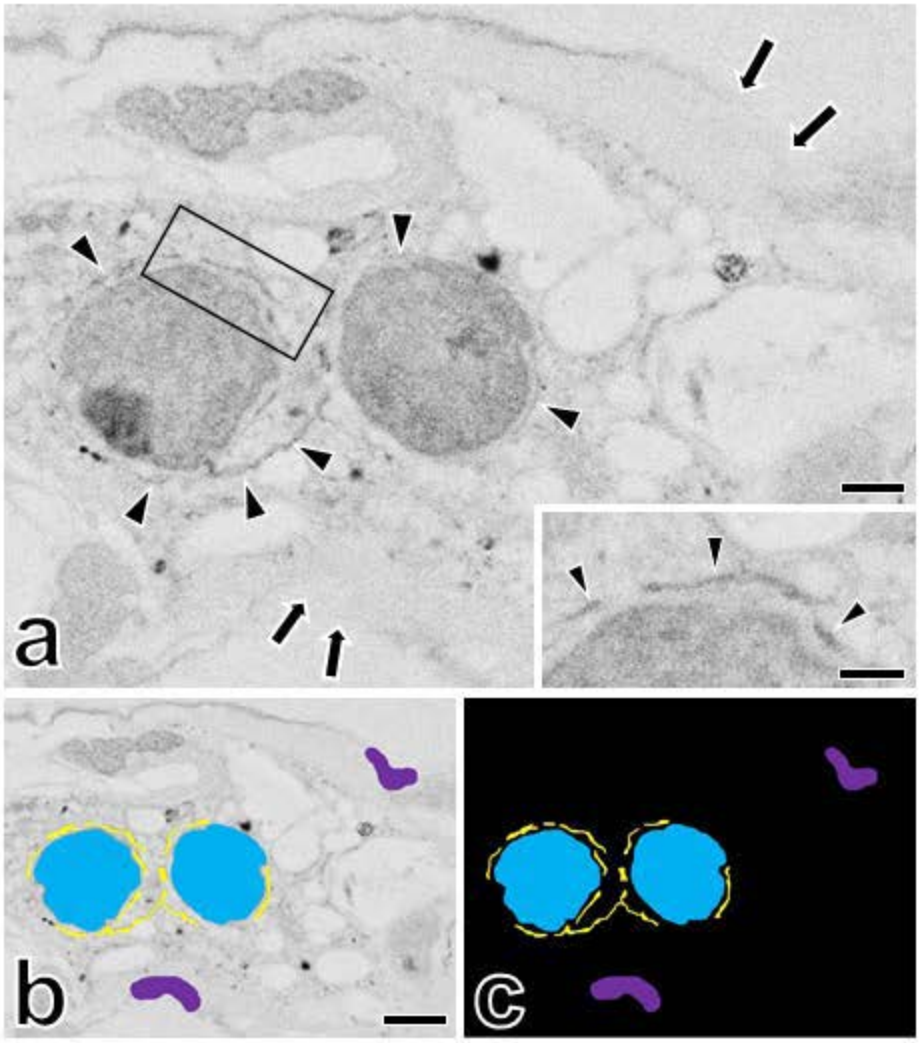

Fig.3

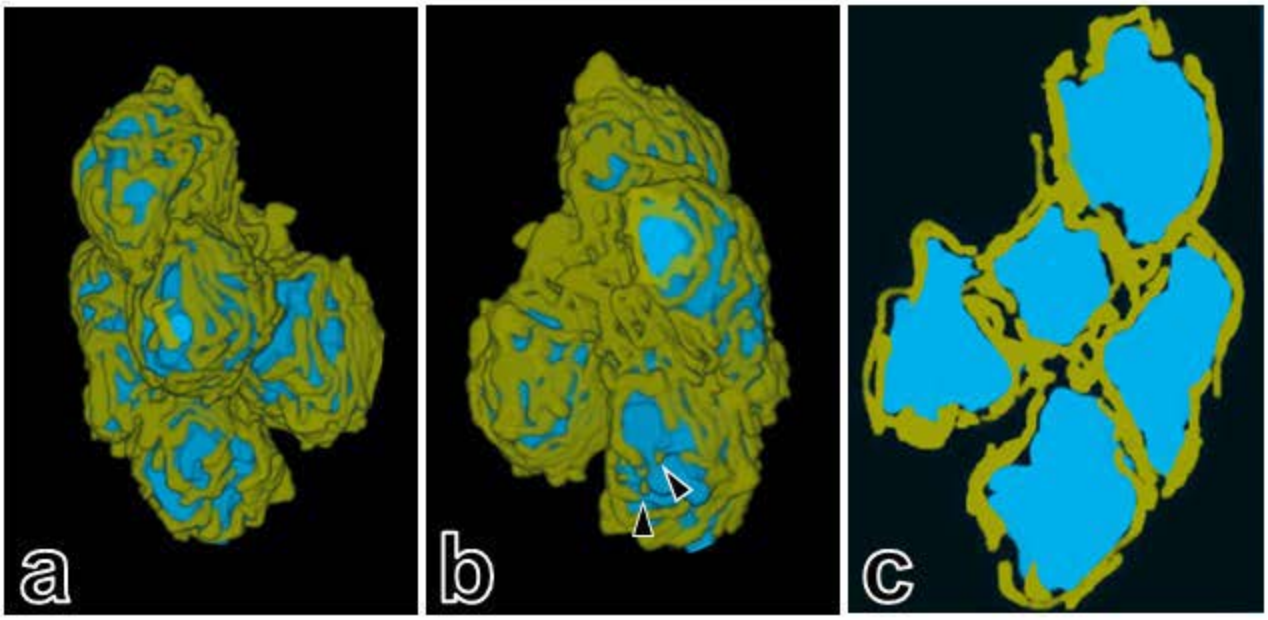

Fig.4

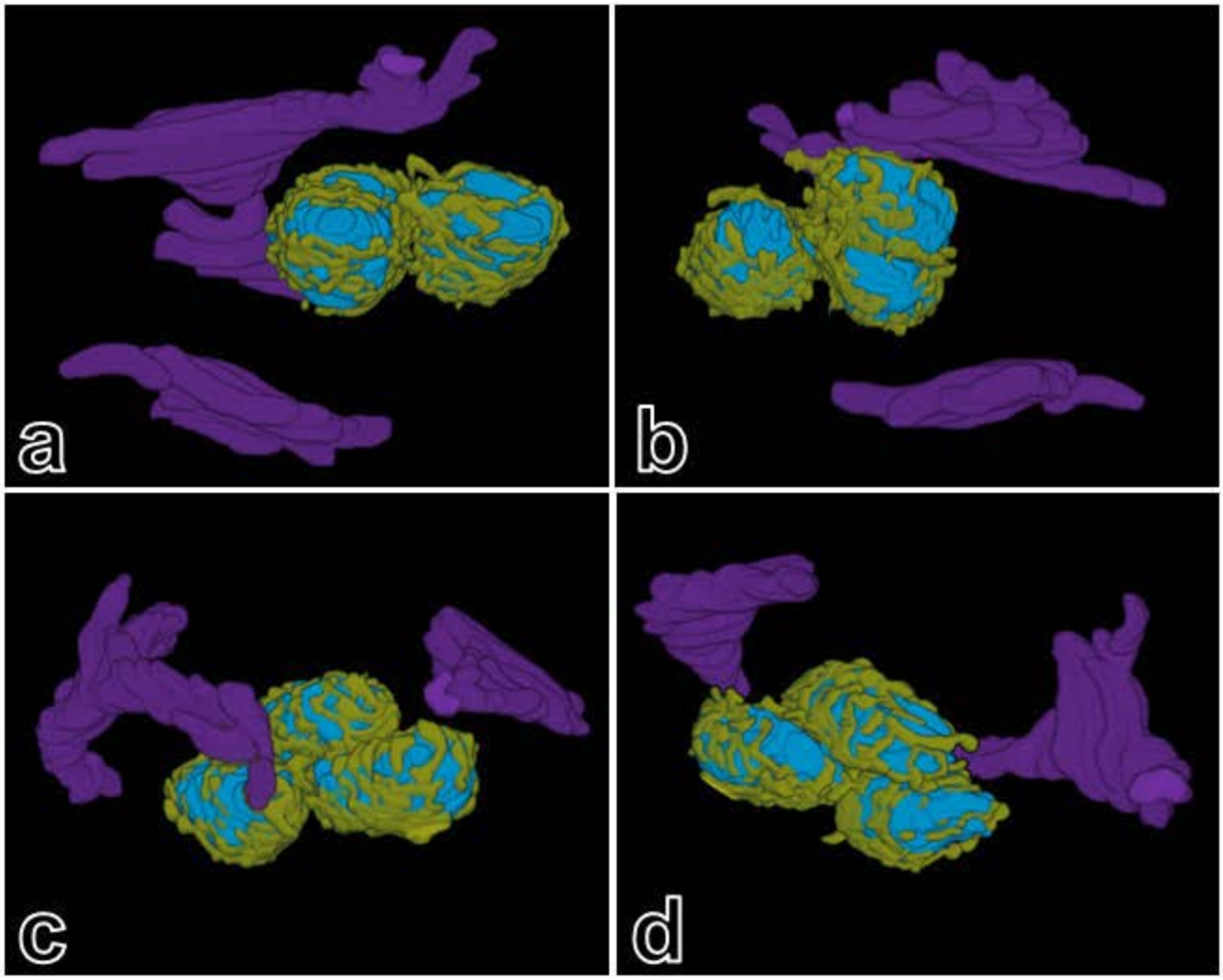

Fig.5